AFRL-RQ-WP-TP-2013-0269

AIRCRAFT DYNAMIC MODES OF A WINGED REUSABLE ROCKET PLANE (PREPRINT)

Barry M. Hellman (AFRL/RQHV) and Brock P. Pleiman (AFRL/RQVI)

Vehicle Technology Branch, High Speed Systems Division (AFRL/RQHV)
Integrated Systems Branch, Aerospace Vehicles Division (AFRL/RQVI)

Mark Street

XCOR Aerospace

SEPTEMBER 2013

AIR FORCE RESEARCH LABORATORY
AEROSPACE SYSTEMS DIRECTORATE
WRIGHT-PATTERSON AIR FORCE BASE, OH 45433-7542
AIR FORCE MATERIEL COMMAND
UNITED STATES AIR FORCE

NOTICE AND SIGNATURE PAGE

*//Signature//

BARRY M. HELLMAN
Aerospace Engineer
Vehicle Technology Branch
High Speed Systems Division

//Signature//

ROBERT MACDERMOTT
Branch Chief
Vehicle Technology Branch
High Speed Systems Division

//Signature//

THOMAS A. JACKSON
Deputy for Science
High Speed Systems Division
Aerospace Systems Directorate

REPORT DOCUMENTATION PAGE

1. REPORT DATE *(DD-MM-YY)*	2. REPORT TYPE	3. DATES COVERED *(From - To)*
September 2013	Journal Article Preprint	01 January 2013 – 30 September 2013

4. TITLE AND SUBTITLE
AIRCRAFT DYNAMIC MODES OF A WINGED REUSABLE ROCKET PLANE (PREPRINT)

5a. CONTRACT NUMBER
In-house

5b. GRANT NUMBER

5c. PROGRAM ELEMENT NUMBER
62201F

6. AUTHOR(S)
Barry M. Hellman (AFRL/RQHV) and Brock P. Pleiman (AFRL/RQVI)
Mark Street (XCOR Aerospace)

5d. PROJECT NUMBER
2404

5e. TASK NUMBER
N/A

5f. WORK UNIT NUMBER
Q05Q

7. PERFORMING ORGANIZATION NAME(S) AND ADDRESS(ES)
Vehicle Technology Branch, High Speed Systems Division (AFRL/RQHV)
Integrated Systems Branch, Aerospace Vehicles Division (AFRL/RQVI)
Air Force Research Laboratory, Aerospace Systems Directorate
Wright-Patterson Air Force Base, OH 45433-7542
Air Force Materiel Command, United States Air Force

XCOR Aerospace
P.O. Box 1163
Mojave, CA 93502

8. PERFORMING ORGANIZATION REPORT NUMBER
AFRL-RQ-WP-TP-2013-0269

9. SPONSORING/MONITORING AGENCY NAME(S) AND ADDRESS(ES)
Air Force Research Laboratory
Aerospace Systems Directorate
Wright-Patterson Air Force Base, OH 45433-7542
Air Force Materiel Command
United States Air Force

10. SPONSORING/MONITORING AGENCY ACRONYM(S)
AFRL/RQHV

11. SPONSORING/MONITORING AGENCY REPORT NUMBER(S)
AFRL-RQ-WP-TP-2013-0269

12. DISTRIBUTION/AVAILABILITY STATEMENT
Approved for public release; distribution unlimited.

13. SUPPLEMENTARY NOTES
PA Case Number: 88ABW-2013-3690; Clearance Date: 03 Dec 2013. This paper contains color.

14. ABSTRACT
This paper presents the results of an effort to quantify the response times for the dynamic modes of a winged reusable rocket plane. The vehicle used in this effort was XCOR Aerospace's Lynx, which is being developed for the suborbital space tourism and microgravity payload market. The effort utilized CART3D and Missile Datcom to estimate the static and dynamic aerodynamics of the Lynx. These inputs were then feed into the "A" matrix of the state space version of the equations of motion.

15. SUBJECT TERMS
dynamic modes, flying qualities, space plane, reusable rockets

16. SECURITY CLASSIFICATION OF:			17. LIMITATION OF ABSTRACT:	18. NUMBER OF PAGES	19a. NAME OF RESPONSIBLE PERSON (Monitor)
a. REPORT Unclassified	**b. ABSTRACT** Unclassified	**c. THIS PAGE** Unclassified	SAR	26	Barry M. Hellman
					19b. TELEPHONE NUMBER *(Include Area Code)* N/A

Aircraft Dynamic Modes of a Winged Reusable Rocket Plane

Barry M Hellman[*] and Brock P. Pleiman.[†]
Air Force Research Laboratory, Aerospace Systems Directorate, WPAFB, OH, 45433

and

Mark Street[‡]
XCOR Aerospace, Mojave, CA, 93502

This paper presents the results of an effort to quantify the response times for the dynamic modes of a winged reusable rocket plane. The vehicle used in this effort was XCOR Aerospace's Lynx which is being developed for the sub-orbital space tourism and microgravity payload market. The effort utilized CART3D and Missile Datcom to estimate the static and dynamic aerodynamics of the Lynx. These inputs were then feed into the "A" matrix of the state space version of the equations of motion.

Nomenclature

CAD	=	Computer Assisted Drawing	psf	=	pounds per square foot
cbar	=	mean aerodynamic chord	Q	=	dynamic pressure
CFD	=	Computation Fluid Dynamics	q	=	pitch rate
C_l	=	Coefficient of Rolling Moment	r	=	yawing rate
C_m	=	Coefficient of Pitching Moment	RCS	=	Reaction Control System
C_n	=	Coefficient of Yawing Moment	RFS	=	Reference Flight System
CRADA	=	Cooperative Research and Development Agreement	S	=	reference area
FAST	=	Future responsive Access to Space Technologies	u_0	=	freestream velocity
g	=	gravitational acceleration	Y	=	Side Force
I_{xx}, I_{yy}, I_{zz}	=	moments of inertia	Z	=	Normal Force
L	=	Roll Moment	α	=	angle of attack
M	=	Pitching Moment	$\dot{\alpha}$	=	change in angle of attack
MDC	=	Missile Datcom	β	=	sideslip angle
N	=	Yawing Moment	θ	=	pitch angle
p	=	rolling rate	λ	=	eigenvalue

I. Introduction

T HE Air Force Research Lab's Aerospace Systems Directorate (AFRL/RQ, the merging of the Air Vehicles and Propulsion Directorates) has been pursuing various efforts to develop the Technology, Processes, and Systems Attributes (TPSA) for next generation affordable and responsive access to space launch systems. These efforts

included the Future responsive Access to Space Technologies (FAST) program[1] and the RBS Pathfinder rocketback flight demonstration program[2]. The FAST program consisted of a demonstrator design, a rapid engine remove and replace demo, a low manpower operations control center, adaptive guidance and control, and lightweight composite structures has nearly completed. The lessons learned were incorporated into what is called the Reference Flight System (RFS) G concept. The RBS Pathfinder program was intended to demonstration in flight the rocketback return to base trajectory[3].

Although the RBS Pathfinder program was canceled after Phase I, the National Research Council in their report about the Reusable Booster System concept[4] endorsed investing in technologies to develop a responsive access to space capability. Current efforts at AFRL/RQ are focused on how affordable and responsive launch TPSAs and concepts can enable the practicality of smaller payloads than those typically launched by the Evolved Expendable Launch Vehicle (EELV) Atlas and Delta vehicles.

Although AFRL/RQ currently doesn't have any funded efforts to develop and demonstrate in flight responsive launch technologies, existing and new partnerships with industry are being formed to leverage private investment in these technology areas. One of these partnerships involves a Cooperative Research and Development Agreement (CRADA) with XCOR Aerospace. This CRADA began in 2008 to focus on development of the Lynx sub-orbital rocket plane[5,6], shown in Figure 1, and has focused on the aerodynamic characteristics of the Lynx. Since the Lynx is being designed to fly through similar environments and the Lynx has similar outer mold line similarities as the RFS concepts from FAST, the efforts under the CRADA will help reduce risk associated with larger launch concepts[7]. Since the Lynx is being designed for multiple flights per day[6], stakeholders can also be shown the practicality and potential utility of responsive rocket powered vehicles.
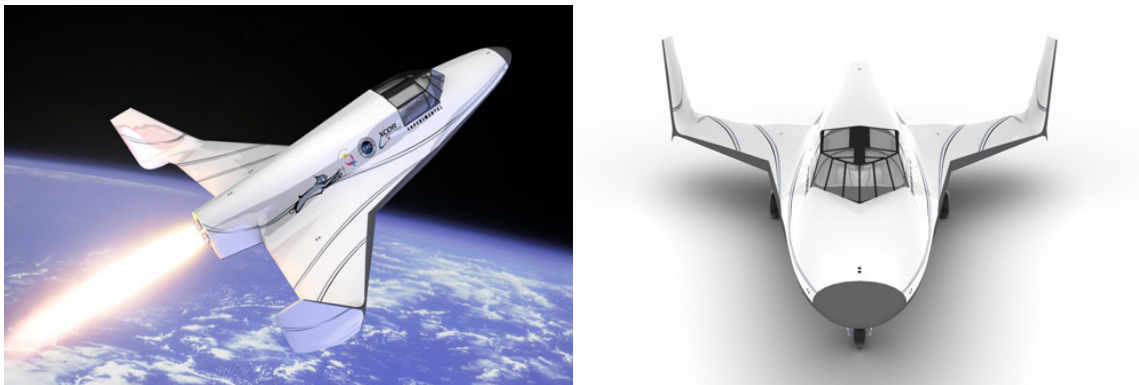
Figure 1. XCOR Aerospace's Lynx Sub-orbital Rocket Plane.

The focus of this paper is to present some of the results from looking at the dynamic flight modes of the Lynx. Since the Lynx is a manned piloted vehicle, this analysis will help designers understand the flying qualities of the vehicle and help with sizing of the vehicle's Reaction Control System (RCS). This analysis approach presented here, which is based on fundamental dynamic mode principles, can easily be applied to other high speed vehicle concepts. Even though most vehicle concepts for responsive launch are unmanned, where traditional flight qualities analysis techniques don't necessarily apply, this approach can help set requirements for design of flight actuation and autonomous control systems.

II. Technical Approach

A. Aerodynamic Analysis

The aerodynamic coefficients that will be used in the dynamic mode analysis were generated using two industry standard tools. For the static aerodynamic analysis, the Euler computational fluid dynamics (CFD) CART3D code developed by NASA Ames Research Center was used[8]. This CFD code utilizes a structured surface grid on top of a "water-tight" Computer Assisted Drawing (CAD) generated outer mold line. The surface grid was very refined and incorporated with a structured volume grid with about 3.8 million cells. Since CART3D is based on the Euler forms of the Navier-Stokes equations[9], there is no viscosity in the solver thus removing the need for a finely resolved

American Institute of Aeronautics and Astronautics

boundary grid to capture the boundary layer. The major shortcomings of this approach include the lack of skin friction drag and the proper placement of shocks on lifting surfaces at transonic speeds. The code will however capture wing tip vortices, base drag, and all surface formed shock waves. Nevertheless, CART3D can be used a mid-fidelity preliminary design tool to make sure a vehicle concepts outer mold has a reasonable amount of confidence in meeting mission requirements. All aerodynamic static derivatives were obtain from these results. The lateral derivatives of Cn_β and Cl_β were based on the linear difference of CART3D analysis between 0º and 5º of slideslip.

For the dynamic aerodynamic analysis, the AFRL and U.S. Army ARMDEC 2008 version of Missile Datcom was used[10]. This tool utilizes a simplified input of vehicle geometry to estimate it aerodynamic properties. A graphic representation of how the Lynx was modeled in Missile Datcom is shown in Figure 2. The fuselage is modeled as simple cylinder with and drooped ogive shaped nose. The wings are modeled as three separate fin sets: the horizontal wing, the dorsal side vertical tail, and the ventral side vertical tail. Missile Datcom makes use of a large empirical database and some physics based methods to allow for very fast lower-fidelity aerodynamic analysis. This tool was used to calculate dynamic aerodynamic coefficients since the only other state of the art tool to estimate these coefficients with some degree of confidence at subsonic, transonic, and supersonic flight conditions is time dependent CFD which can take days just to get one flight conditions. MDC can analyze the entire flight envelope of the Lynx in less than a minute. Due to limited resources available at AFRL for this effort, the lower-fidelity method was used.
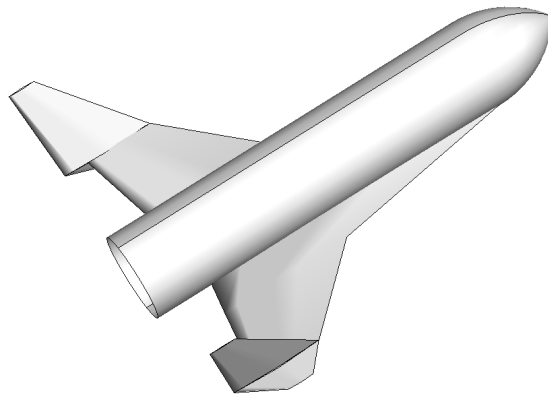
Figure 2. Graphical Representation of How the Lynx was Modeled in Missile Datcom.

The static aerodynamics from CART3D and MDC were compared upfront to help understand any differences between the tools. Since CART3D is considered a higher fidelity analysis tool, those static coefficients were assumed to be "truth" for the sake of this effort. Figure 3 through Figure 6 compare the results from these two tools. At each flight condition, MDC consistently showed a reduced lift coefficient and large differences in pitching, yawing, and rolling moment coefficient. After discussion with William Blake of AFRL/RQQD (who has been involved with MDC's development for many years), it was determined that the largest source of error between the two aerodynamic analysis tools was that MDC doesn't account for the geometric connection between the horizontal wing and the vertical tails on the wing tips. MDC assumes that each wing/fin is independent of all other wings/fins. MDC also assumes that the lift of the horizontal wing goes to zero at the tip with an elliptical lift distribution, the typical properties of a 3D wing. The vertical tail allows the wing to retain some of its lift and the wing tip since it acts like a plate allowing for more "2D Wing" properties. Since the wing is swept, this lift discrepancy will cause the center of pressure to be different resulting in aerodynamic moment differences.

To obtain a higher confident result for the dynamic derivatives, MDC was rerun using adjusted moment reference points to match the moment values from CART3D (dynamic mode analysis was only conducted at those flight conditions analyzed in CART3D). The center of pressure was moved in the axial direction to match the static pitching moment to obtain the longitudinal dynamic derivatives. The center of pressure was then moved in the axial direction to match the static yawing moment and in the vertical direction to match the static rolling moment to obtain the lateral dynamic derivatives. MDC takes the static moments and does perturbations around those values to get the dynamic derivatives so the static moment value needs to be as accurate as possible. For the dynamic mode analysis, only the dynamic derivatives were used from these MDC adjusted analyses.

American Institute of Aeronautics and Astronautics

For the dynamic mode calculations in MDC, only the Cl_p (roll moment with roll rate) derivative requires the lift coefficient. With the adjusted analysis in MDC, using a lower coefficient will provide a more conservative value of Cl_p, i.e. a larger value.

Figure 3. Comparison of Static Aerodynamics from CART3D and MDC for Mach 0.3.

American Institute of Aeronautics and Astronautics

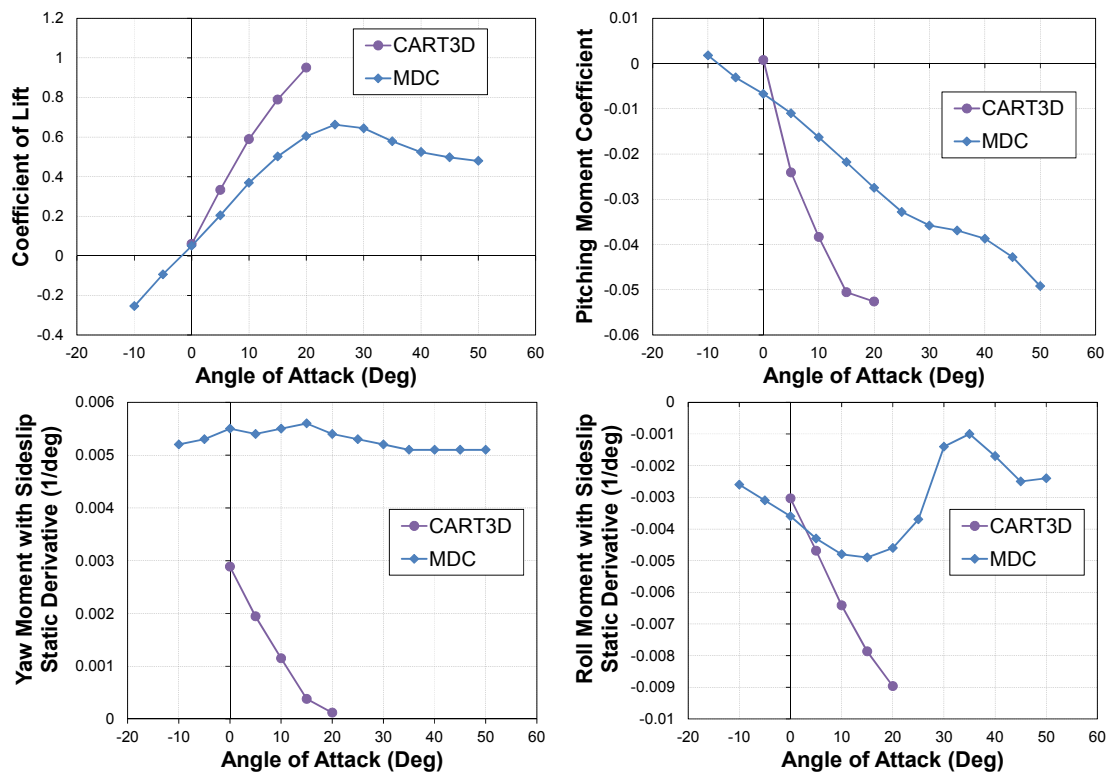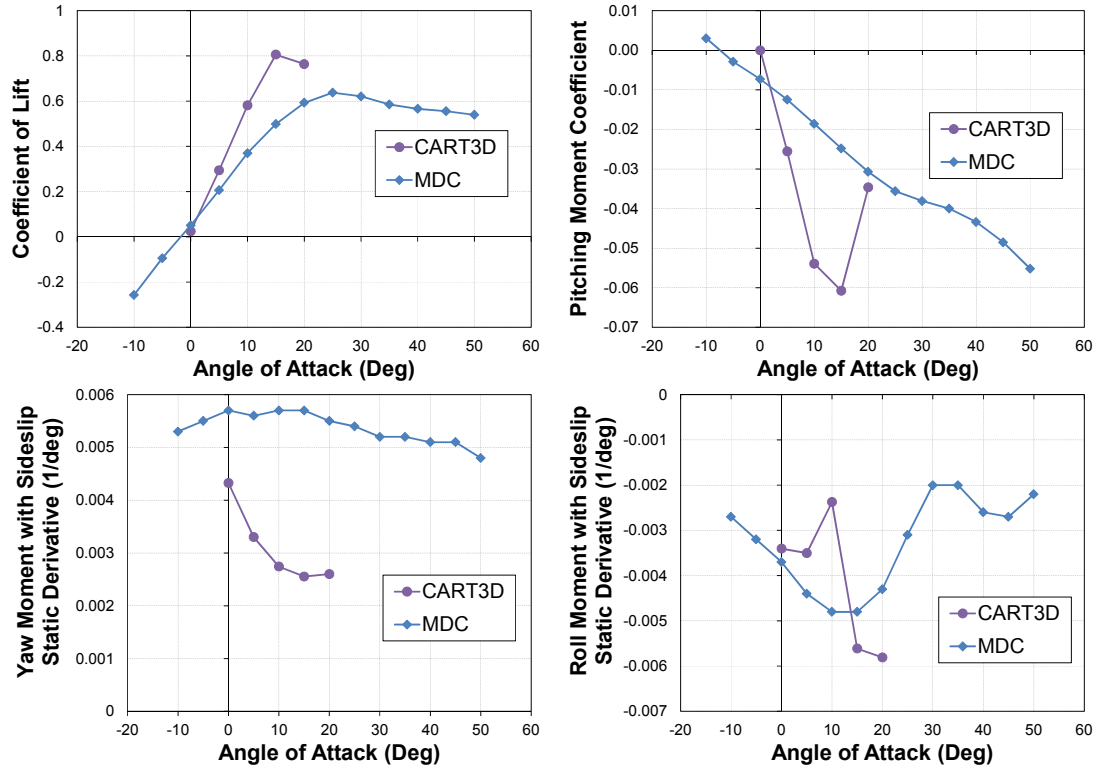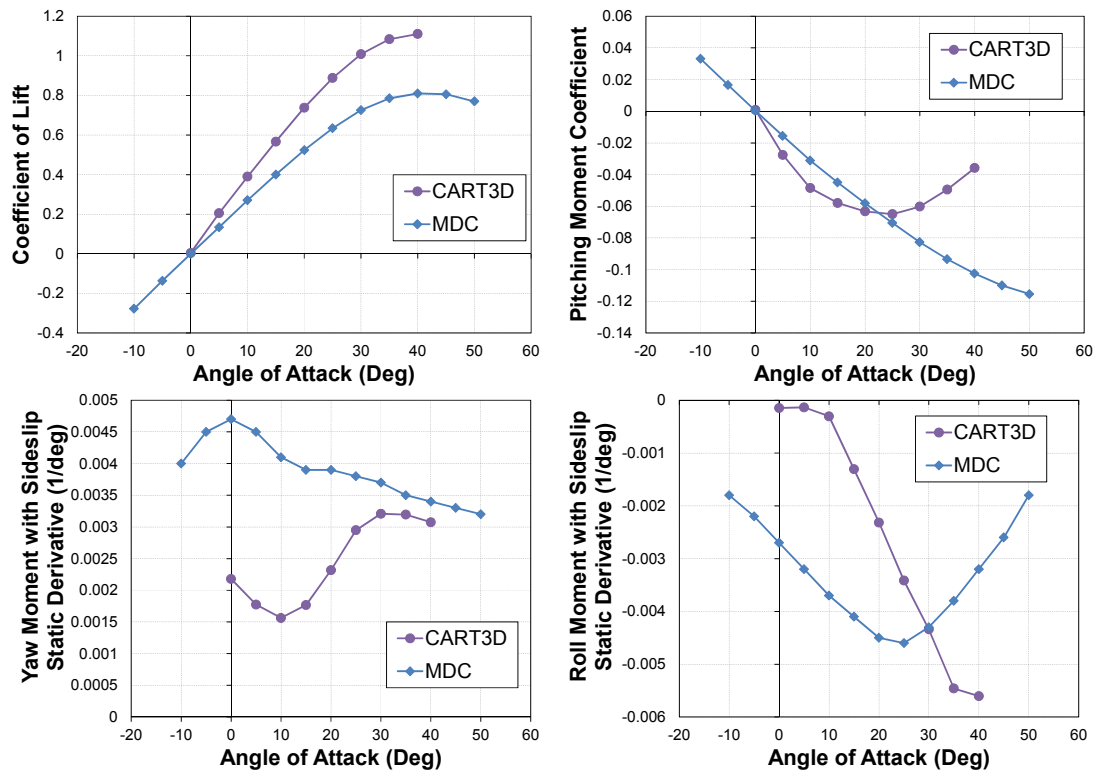Approved for public release; distribution unlimited.

Figure 4. Comparison of Static Aerodynamics from CART3D and MDC for Mach 0.5.

Figure 5. Comparison of Static Aerodynamics from CART3D and MDC for Mach 1.5.

American Institute of Aeronautics and Astronautics

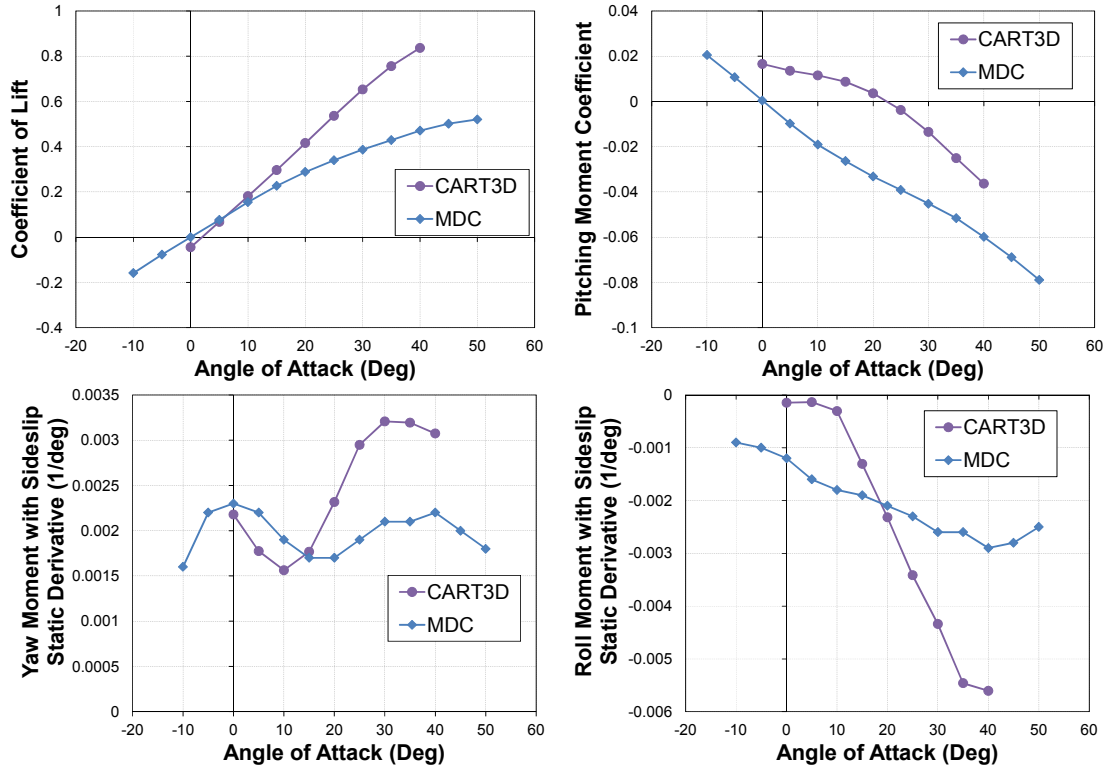Approved for public release; distribution unlimited.

Figure 6. Comparison of Static Aerodynamics from CART3D and MDC for Mach 3.0.

B. Dynamic Mode Analysis

There are traditionally 5 rigid body dynamic modes for an aircraft in flight which are derived from the aircraft equations of motion in state-space form. The two longitudinal modes are phugoid and short period mode. The phugoid mode is an oscillatory energy tradeoff between altitude and velocity. This mode occurs over longer periods and can easily be damped by a pilot or simple autonomous control system. The phugoid mode was not analyzed in this effort. The short period mode is an oscillatory difference in variation between the vehicle's angle of attack and pitch angle[11]. This mode occurs over short periods with airspeed and altitude nearly constant. Using that assumption, the eigenvalues (λ) can be calculated from equation 1 to analyze the short period mode[12]. The force and moment terms in that equation are calculated from equations 2 through 8. According to typical aircraft mode analysis, the short period is oscillatory meaning that the eigenvalues for short period will be a complex pair. Those values not defined below are listed in the nomenclature section of this paper. These equations show that the short period mode is a function of dynamic pressure, velocity, the vehicle's longitudinal aerodynamics, the dimensions used to make the coefficients (reference area and length), and the vehicle's moment of intertia in the x-z directions.

$$\lambda_{1,2} = \frac{M_Q + M_{\dot{\alpha}} + \frac{Z_\alpha}{U_0}}{2} + \frac{\left(\left(M_Q + M_{\dot{\alpha}} + \frac{Z_\alpha}{U_0} \right)^2 - \left(4 * M_Q * \frac{Z_\alpha}{U_0} - M_\alpha \right) \right)}{2} \tag{1}$$

$$Z_w = -G * \frac{(C_{L_\alpha} + C_D) * q * S}{mass * U_0} \tag{2}$$

$$Z_\alpha = U_0 * Z_w \tag{3}$$

American Institute of Aeronautics and Astronautics

$$M_Q = C_{M_Q} * \left(\frac{cbar}{2 * U_0}\right) * \frac{q * S * cbar}{I_{yy}} \qquad (4)$$

$$M_w = \frac{C_{M_\alpha} * Q * S * cbar}{I_{yy} * U_0} \qquad (5)$$

$$M_\alpha = U_0 * M_W \qquad (6)$$

$$M_{\dot{w}} = Cmad * \left(\frac{cbar}{2 * U_0}\right) * \frac{(q * S * cbar)}{U_0 * I_{yy}} \qquad (7)$$

$$M_{\dot{\alpha}} = U_0 * M_{\dot{w}} \qquad (8)$$

The lateral modes are spiral, roll, and dutch roll. Spiral mode is non-oscillatory and is a "…yawing motion with some roll"[11]. The spiral mode can be unstable in aircraft but usually is slow enough that it can typically be compensated by the pilot or control system and is depicted in Figure 7. The roll mode is another non-oscillatory mode that involves a "…pure rolling motion around the vehicle's x-stability axis". The dutch roll mode is oscillatory with " … a rolling and yawing motion with some sideslipping" and is depicted in Figure 8.
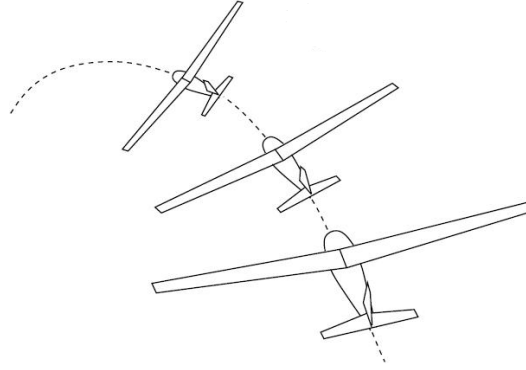
Figure 7. Depiction of Spiral Mode[12,13] (picture shows an unstable mode).
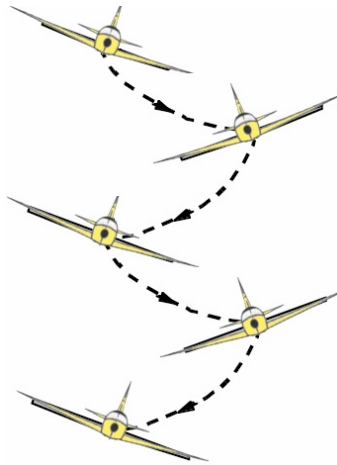
Figure 8. Depiction of Dutch Roll Mode[1214].

Aircraft control text books, including those referenced in this paper, present simplifications of each of these three modes. However, since the Lynx is not a traditional aircraft flying at a wide range of flight conditions and higher angles of attack, these approximations were not used to analyze those modes. The state space "A" matrix for the

7

American Institute of Aeronautics and Astronautics

Approved for public release; distribution unlimited.

lateral equations of motion was used to calculate the eigenvalues for each mode. This matrix along with the equations that make up its components are in equations 9 through 17. A typical set of eigenvalues from this matrix plotted on a real-imaginary axis is shown in Figure 9. These two pictures show all eigenvalues to have negative real parts, indicating stability, but they can fall on the positive real side. These equations show that the lateral modes area a function of vehicle pitch angle, dynamic pressure, velocity, the vehicle's lateral aerodynamics, the dimensions used to make the coefficients (reference area and length), vehicle's mass, and the vehicle's moment of inertia in the x-y and y-z directions.

$$
\begin{array}{|c|c|c|c|}
\hline
\dfrac{Y_\beta}{U_0} & \dfrac{Y_p}{U_0} & -\left(1 - \left(\dfrac{Y_r}{U_0}\right)\right) & \dfrac{g}{U_0} * \cos(\theta) \\
\hline
L_\beta & N_p & L_r & 0 \\
\hline
N_\beta & N_p & N_r & 0 \\
\hline
0 & 1 & 0 & 0 \\
\hline
\end{array}
\tag{9}
$$

$$
Y_\beta = \frac{Q * q * S * C_{y_\beta}}{mass} \tag{10}
$$

$$
Y_p = \frac{Q * S * span * C_{y_p}}{2 * mass * U_o} \tag{11}
$$

$$
Y_r = \frac{Q * S * span * C_{y_r}}{2 * mass * U_o} \tag{12}
$$

$$
N_\beta = \frac{Q * S * span * C_{n_\beta}}{Izz} \tag{13}
$$

$$
N_p = \frac{Q * S * span^2 * C_{np}}{2 * Izz * U_0} \tag{14}
$$

$$
N_r = \frac{Q * S * span^2 * C_{nr}}{2 * Izz * U_0} \tag{15}
$$

$$
L_\beta = \frac{Q * S * span * C_{lB}}{Ixx} \tag{16}
$$

$$
L_p = \frac{Q * S * span^2 * C_{lp}}{2 * Ixx * U_0} \tag{17}
$$

$$
L_r = \frac{Q * S * span^2 * C_{lr}}{2 * Ixx * U_0} \tag{18}
$$

American Institute of Aeronautics and Astronautics

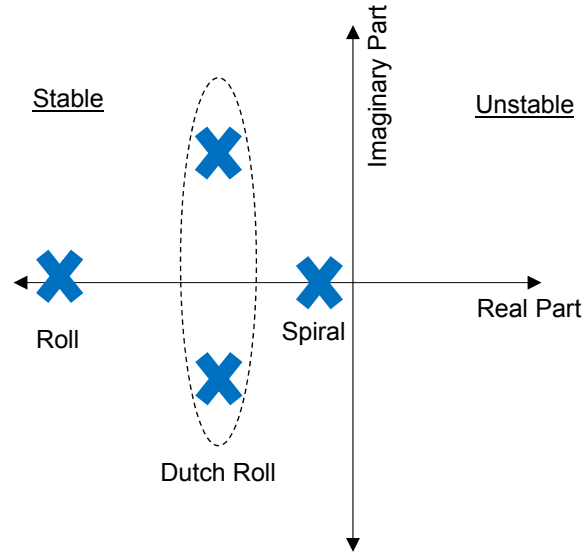Approved for public release; distribution unlimited.

Figure 9. Typical Layout of Eigenvalues from Lateral "A" Matrix.

C. Presentation of Stability of Dynamic Modes

This paper uses a unique approach of presenting the amount of stability or instability of the four dynamic modes. The time to half (for a stable mode) or time to double (for an unstable mode) are presented for each mode in charts laid out like Figure 10. Points above the x-axis show the mode to be unstable while points below are stable. The charts will show points for various dynamic pressures at constant Mach numbers. The x-axis will be the angle of attack. The time to half or time to double is calculated using equation 19.

Figure 10. Method of Plotting Time Responses of Dynamic Modes.

$$Time\ to\ Double\ |\ Time\ to\ Half\ = \frac{ln(2)}{\text{Real}(\lambda)}$$

If Real $(\lambda) < 0$, then it is Time to Half (stable)

If Real $(\lambda) > 0$, then it is Time to Double (unstable)

(19)

American Institute of Aeronautics and Astronautics

III. Results

A. Dynamic Derivatives

The following plots show the dynamic derivatives calculated through the method described above. It should be noted that all $C_{M\ alpha\text{-}dot}$ from MDC shows all values the same at across angles of attack. For every Mach number, the sign for each derivative is the same along with the basic shape of each curve.
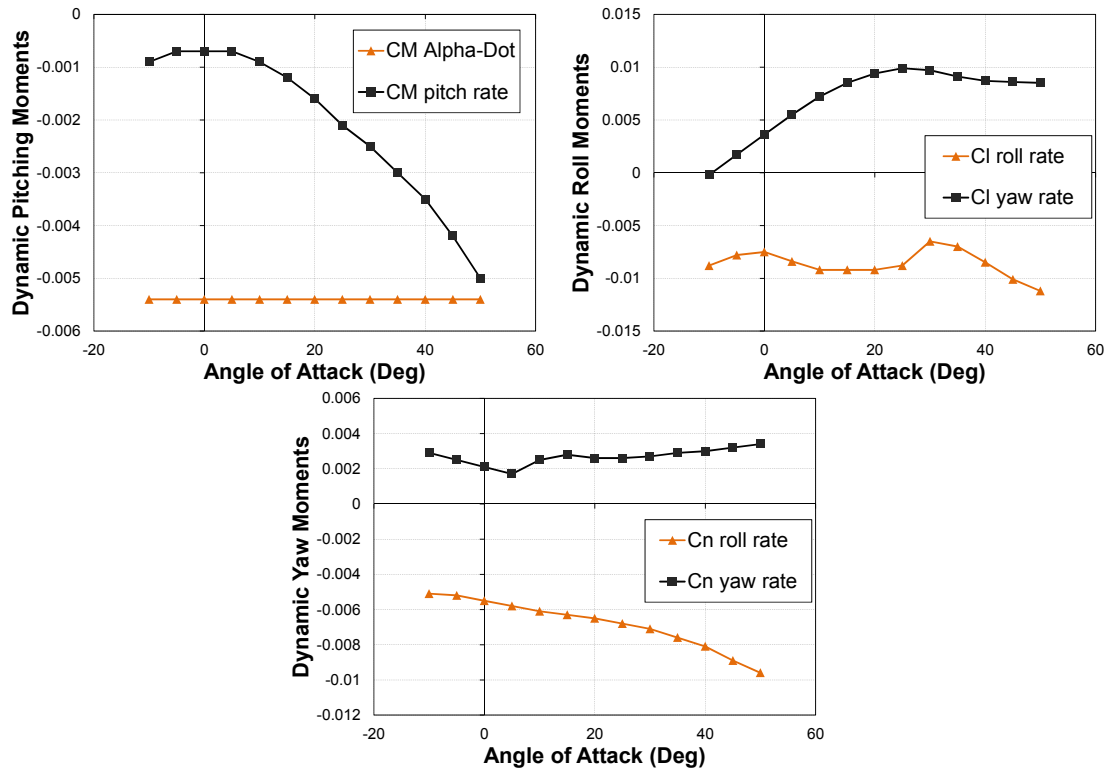
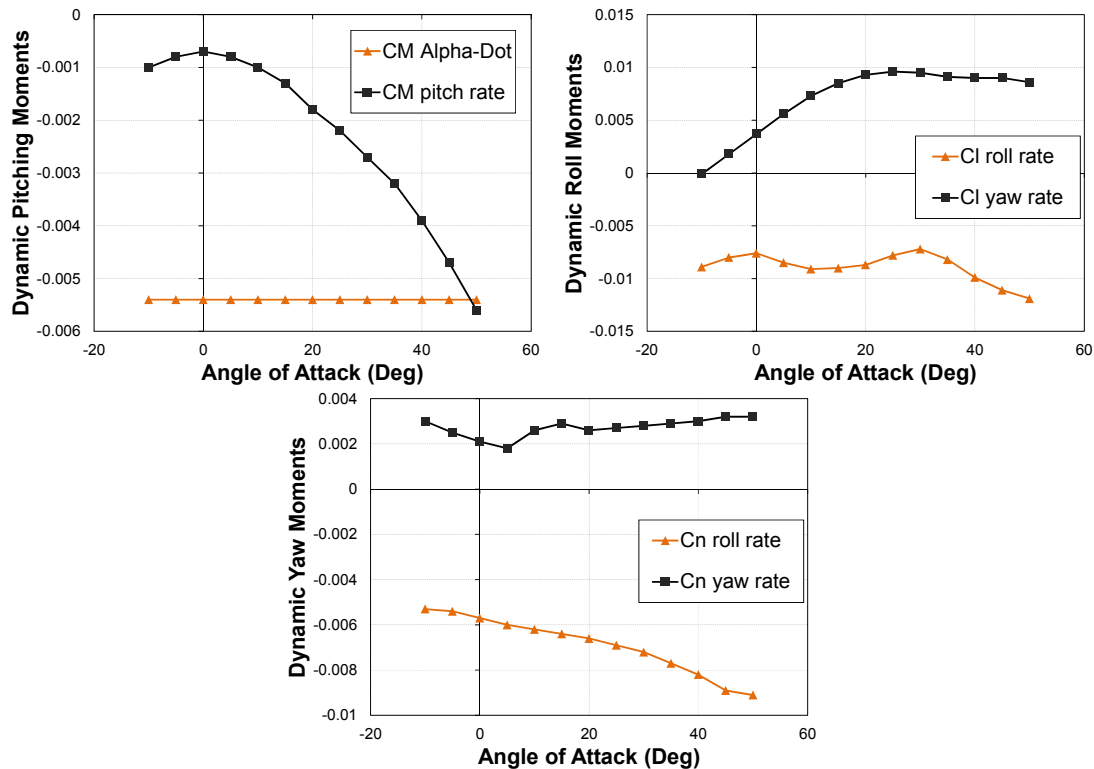

Figure 11. Dynamic Derivatives for Mach 0.3.

American Institute of Aeronautics and Astronautics

Approved for public release; distribution unlimited.

Figure 12. Dynamic Derivatives for Mach 0.5.
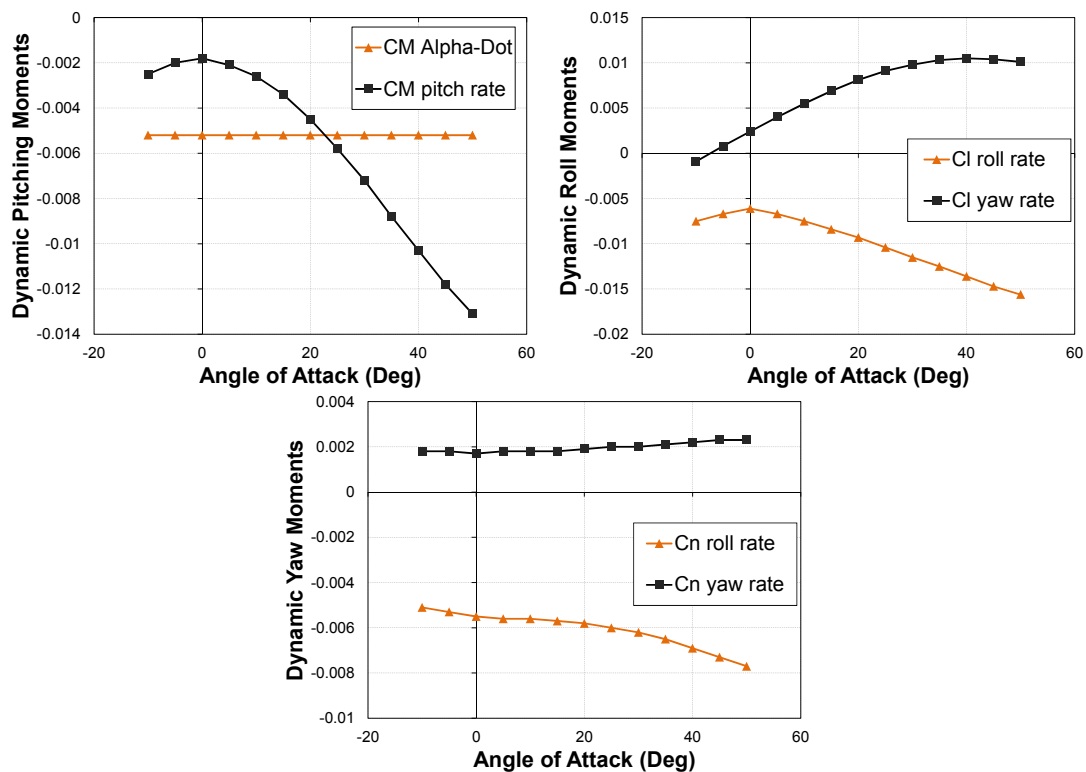
Figure 13. Dynamic Derivatives for Mach 1.5.

American Institute of Aeronautics and Astronautics

Approved for public release; distribution unlimited.
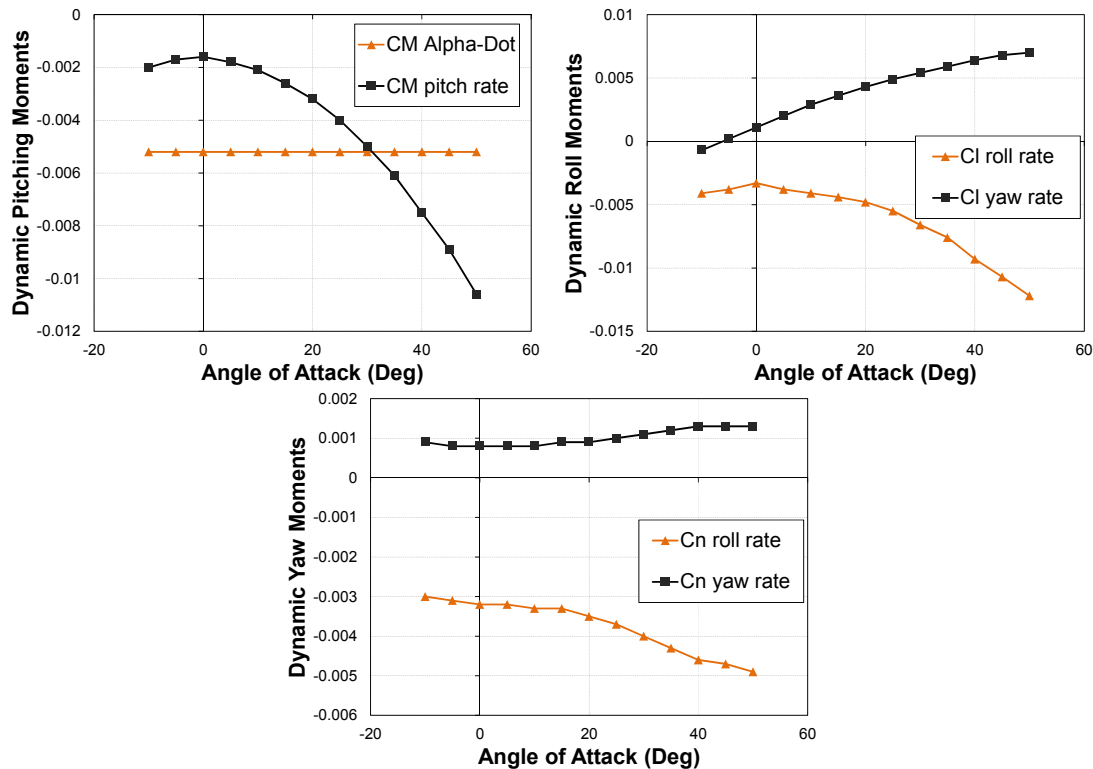
Figure 14. Dynamic Derivatives for Mach 3.0.

B. Dynamic Mode Time to Half / Time to Double Results

The results in this section show the time to half and time to double response times for short period, roll, spiral, and dutch roll dynamic modes. As discussed above, the charts show the response times for different Mach numbers at angles of attack that could be experienced in flight. In each of these charts, times are shown for dynamic pressures of 50, 150, and 250 psf.

Figure 15 shows the response times for short period mode at a range of Mach numbers and angles of attack. A commonality for all the results is all flight conditions are stable and that the higher the dynamic pressure at a particular angle of attack, the more stable the mode is. At subsonic speeds, the vehicle stalls above 15º of attack. At Mach 1.5, the vehicle goes unstable in pitch above 25º angle of attack. Since those flight conditions are not going to be experienced by the Lynx, they aren't presented here. At the supersonic Mach numbers There is a significant increase in stability going increasing the dynamic pressure from 50psf to 150psf. These results help to show where RCS thrusters may be needed until the dynamic pressure is high enough to damp out this mode. The results shown are for angles of attack relevant for the Lynx's flight.

The basic way to assess the longitudinal flying qualities is to look at the damping ratio[11,12]. Since the rules of thumb from textbooks are really only valid for typical aircraft, the damping ratios are presented for subsonic speeds. To have Level 1 and Level 2 flying qualities, the damping ratio needs to be above 0.25 and 0.2 depending on type of flight phase. Most of the conditions presented at least meet the Level 2 parameters. At Mach 0.5, the 50 psf damping ratios are a little low but the vehicle won't be flying at that dynamic pressure anyway. These results shouldn't force the reader into any conclusions as they are just rules of thumb and are for aircraft that are significantly different than the Lynx.

The lateral results are shown in Figure 17 through Figure 20. The same angles of attack for different flight conditions. shown for short period mode, are plotted here. Again the same trend is seen where the higher dynamic pressure increases the mode's stability. The roll and spiral modes are plotted versus angles of attack while the dutch roll mode is plotted versus Mach number. This was determined to be the best way to present the data.

For roll mode, each flight condition is stable with the subsonic points being more stable than supersonic. Stability for this mode increases with angle of attack.   Similar to short period mode, the stability increases significantly with dynamic pressure, especially going from 50 psf to 150 psf. To understand the lateral flying

American Institute of Aeronautics and Astronautics

qualities of this mode, the basic method in references 11 and 12 is to look at the time constant (which is the reciprocal of the eigenvalue). Figure 18 shows the time constants for the subsonic speeds and they are all less than 1 second which means based on these results that the Lynx should have level 1 flying qualities for roll mode at these conditions.

For spiral mode, the times to double or times to half are shown in Figure 19. Aircraft can often have unstable spiral modes as long as the mode's time to double is slow enough for the pilot to respond. The results based on the analysis discussed in this paper for spiral mode shows that, depending on the Mach number, the spiral mode can be unstable at 5º and 10º angle of attack. Everywhere else it is stable. For the most part, stability increases or remains about the same with angle of attack at the supersonic speeds. Like the other modes, the stability also increases for the most part with dynamic pressure. The lateral flying quality parameters for spiral mode in reference 12 are based on a minimum time to double. Based on this data, it can be inferred that if the mode is stable at a certain flight condition, the vehicle has Level 1 flying qualities. Looking at the subsonic unstable flight conditions, all of the points are greater than 20 seconds time to double indicating Level 1 flying qualities for spiral mode. The supersonic unstable points have very large times to double, in the 100's of seconds. While these textbook flying quality rules of thumb for the Lynx at supersonic speeds likely aren't appropriate, nevertheless, these results indicate there isn't much risk in spiral mode at supersonic speeds.

The dutch roll responsive times are shown in Figure 20. These response times are plotted versus Mach number for a constant angle of attack. For subsonic speeds and at 0º angle of attack, which is relevant for the gliding and landing portion of the flight, the mode is stable. It is interesting to note, that the stability decreases some when the flow begins to be compressible (i.e. greater that mach 0.3) and begins to be more stable into the transonic flight regime. At supersonic speeds and higher angles of attack, there is a large increase in stability going from 50psf to 150psf. This indicates that at the lower q, RCS thrusters likely be needed to help maintain control. The lower q will happen during re-entry so RCS usage is expected. For both angles of attack presented, the stability decreases slightly with Mach number. To understand the dutch roll mode flying qualities, reference 12 uses minimum damping ratio, natural frequency, and their product (which is the absolute value of real part of the dutch roll eigenvalue complex pair). Using the times to double minimum (based on the minimum product of damping ratio and natural frequency), the results indicate that Lynx has at least level 2 flying qualities subsonically with the higher dynamic pressure being near or meeting the Level 1 parameter. Again, these rules of thumb aren't being applied to the supersonic conditions.

Since the lateral dynamic modes are also a function of the vehicle's pitch angle, comparisons to 15º and 30º pitch angle are shown in Figure 21. Since the A matrix applies the cosine function to the pitch angle, it doesn't matter if the angle is positive or negative. These comparisons show that there isn't much change in response time based on pitch angle.
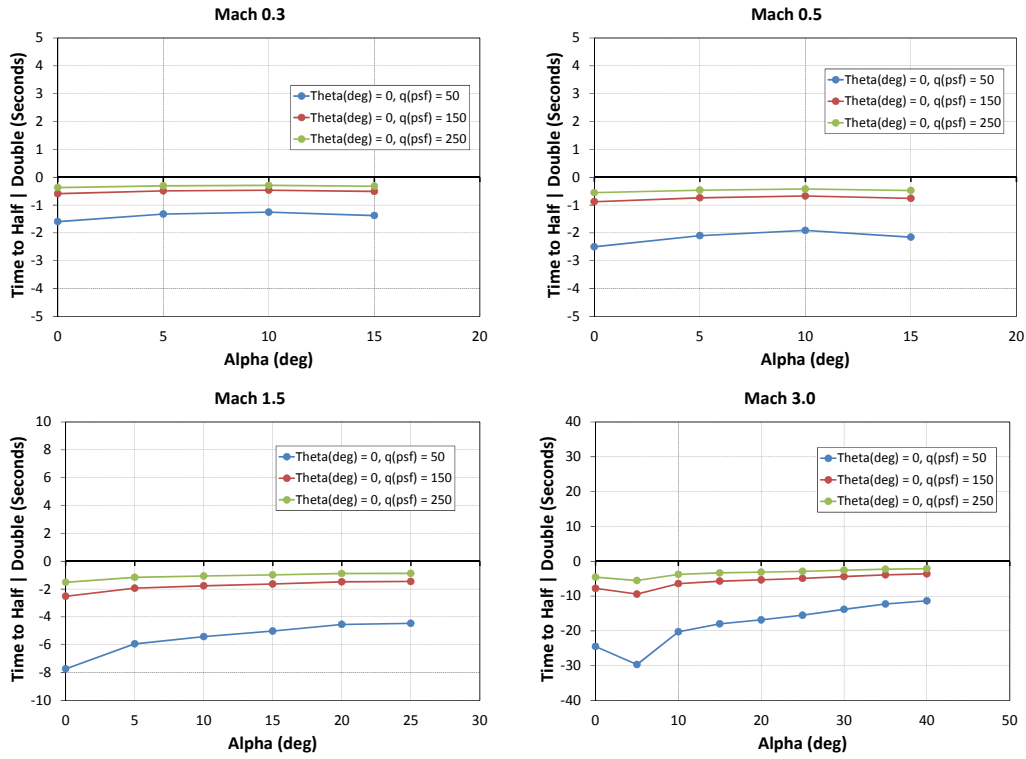
American Institute of Aeronautics and Astronautics

Approved for public release; distribution unlimited.

Figure 15. Short Period Mode Response Times.
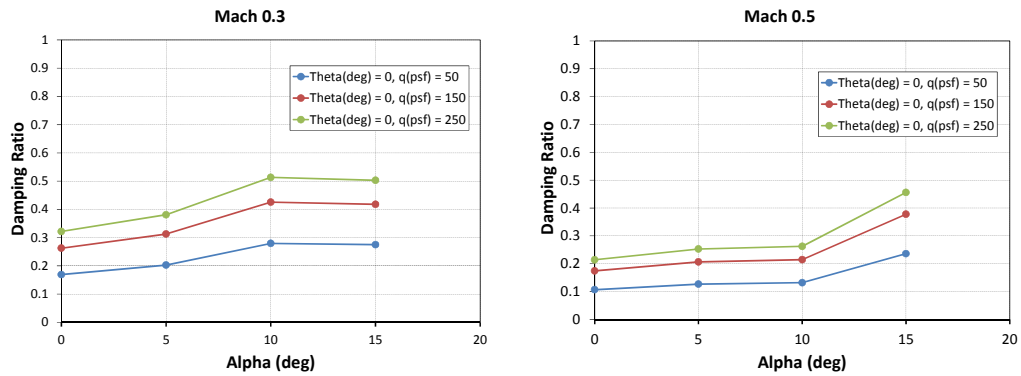
Figure 16. Short Period Mode Damping Ratios for Subsonic Speeds.

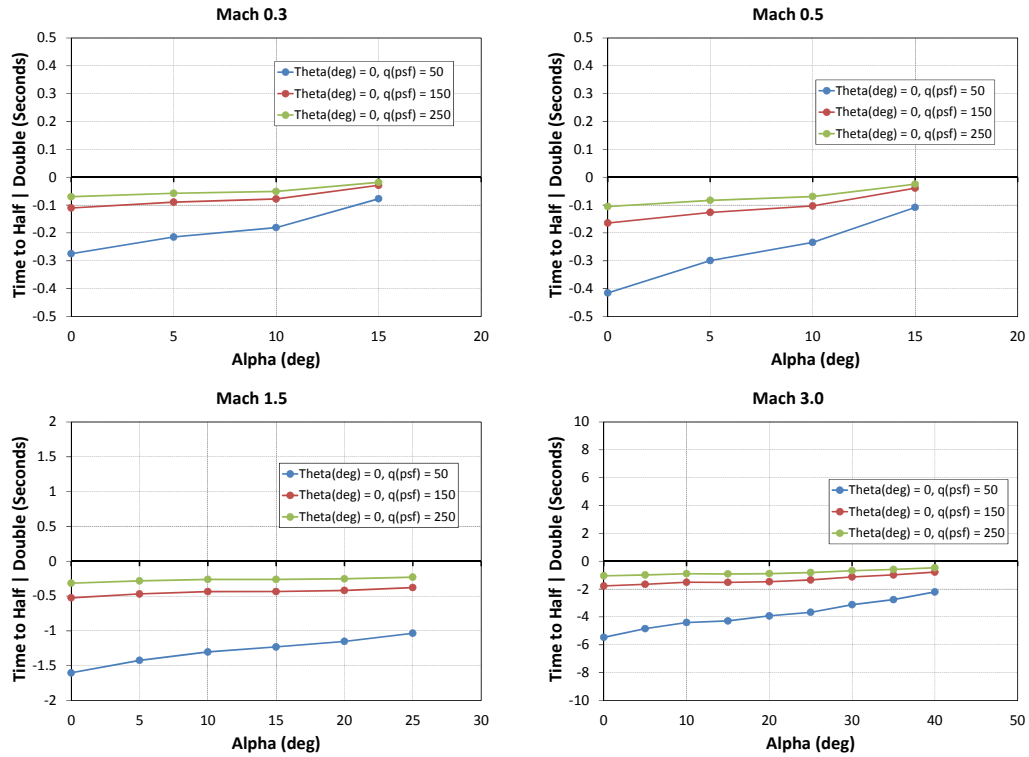American Institute of Aeronautics and Astronautics

Approved for public release; distribution unlimited.

Figure 17. Roll Mode Response Times.
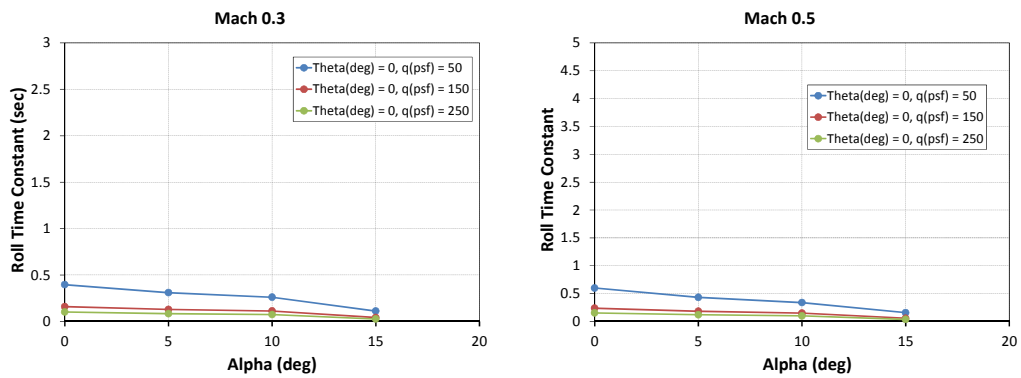
Figure 18. Roll Mode Subsonic Time Constants.

American Institute of Aeronautics and Astronautics

Approved for public release; distribution unlimited.
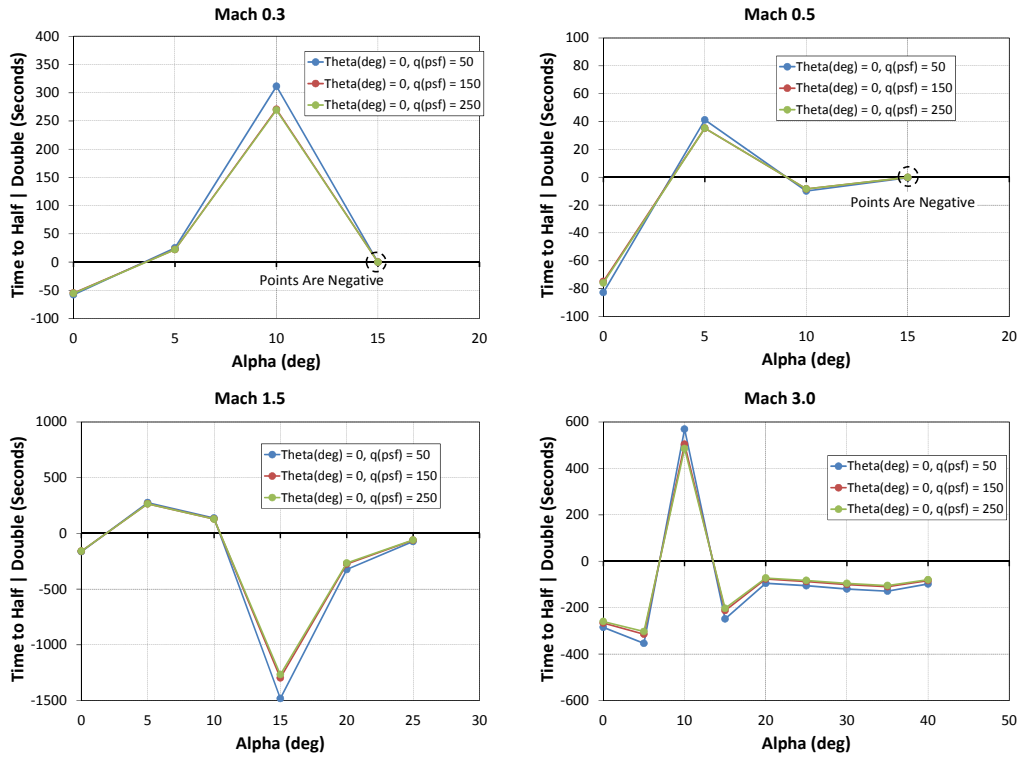
Figure 19. Spiral Mode Response Times.
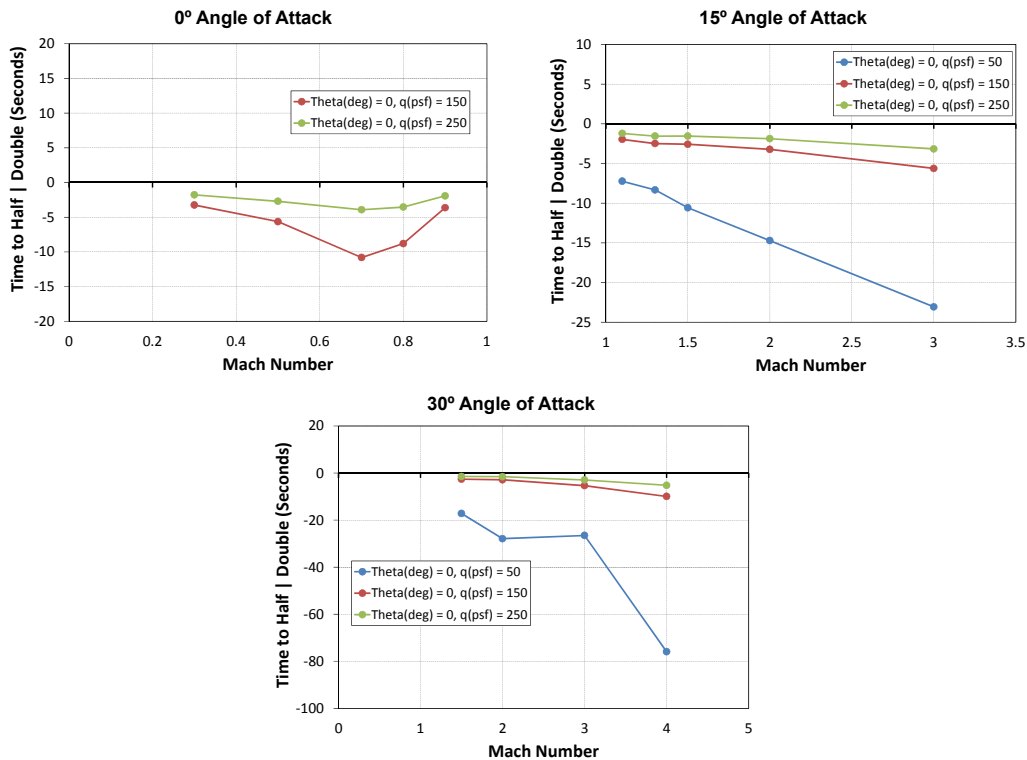
Figure 20. Dutch Roll Mode Response Times.

American Institute of Aeronautics and Astronautics

Table I. Dutch Roll Flying Quality Rules of Thumb from Reference 12.

Flying Quality Level	Minimum (damping ratio * natural frequency)	Time to Half (sec)
1	0.35 or 0.15 (depending on flight phase)	1.98 or 4.62
2	0.05	13.86
3	--	--
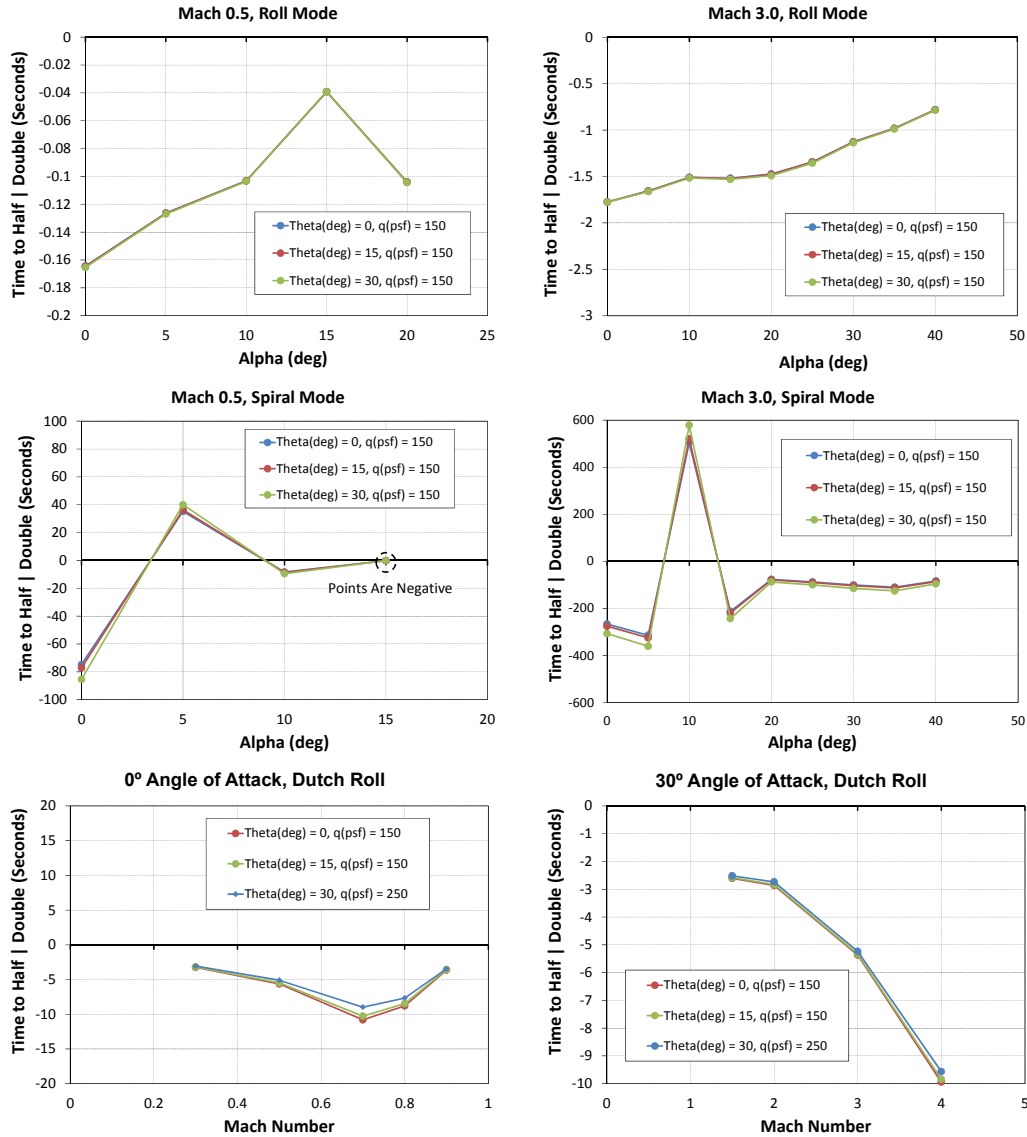
Figure 21. Comparisons of Dynamic Modes at Various Pitch Angle (θ).

American Institute of Aeronautics and Astronautics

Approved for public release; distribution unlimited.

IV. Conclusions

This paper presented a method for conceptual/preliminary dynamic modes analysis of a reusable rocket plane. The vehicle used in this method was XCOR Aerospace's Lynx sub-orbital rocket plane. This analysis was done to see if there are any flight conditions that could cause some flying qualities concerns. The techniques can also be applied to unmanned vehicle to see if there are any flight conditions that would stress the responsiveness of an autonomous flight control system.

The design tool used for dynamic aerodynamic analysis, Missile Datcom, is one the best tools in the industry to do this analysis across many flight conditions. However, due to the unique design of the Lynx, especially with the larger vertical tails, the method of using MDC, had to be "tweaked" to compensate for a lack of some missing physical princples. Of course this can bring into question the results so the analysis presented here should only be considered a starting point towards understanding the flying qualities of the Lynx. Either upgrades to MDC or adding in dynamic analysis into CART3D[15] (not yet available) would be good next steps to build confidence the results.

This effort did produce promising results from not using lateral mode approximations but directly working with the eigenvalues. For the 4 dynamic modes, the Lynx is showing promising flying qualities. The methods used are good for preliminary design but the results need to be taken with the appropriate caution due to their fidelity level and built in assumptions. The method shown can easily applied to various reusable rocket powered vehicles early in the design phase to identify potential controllability concerns. Since the Lynx will be flying at steep pitch angles, the relatively low sensitivity of the lateral modes to that parameter helps reduce controllability risk. Future efforts of the CRADA involve modeling the Lynx in AFRL's Large Amplitude Multi-mode Aerospace Research Simulator (LAMARS), shown in Figure 22, to get a better handle on flying qualities[16,17].

Figure 22. Photograph of AFRL's LAMARS Simulator.

Acknowledgments

American Institute of Aeronautics and Astronautics

References

[1] Jordan, Holly H. "FAST program seeks to mature hypersonic air vehicles and space launch technologies". http://www.wpafb.af.mil/news/story.asp?id=123080301

[2] "Reusable Booster System (RBS) Flight and Ground Experiments" BAA-11-01-PKV www.fbo.gov

[3] Hellman, B., et.al. "Critical Flight Conditions of Operational Rocketback Trajectories." AIAA-2012-5208.

[4] *Reusable Booster System Review and Assessment (2012).* The National Academies Press.

[5] Press Release: "XCOR Aerospace Tests Lynx Aerodynamic Design in USAF Wind Tunnel." July 24, 2009. http://xcor.com/press/2009/09-07-24_XCOR_tests_lynx_aerodynamics_in_USAF_wind_tunnel.html

[6] "About Lynx" xcor.com/lynx

[7] Hellman, B., McKee, K., Street, M., Remillard, Craig. "Advancing ORS Technologies and Capabilities with a Space Tourist Suborbital Vehicle." AIAA-2009-6690.

[8] "Cart3D." http://people.nas.nasa.gov/~aftosmis/cart3d/

[9] Anderson, John D. Jr., *Fundamentals of Aerodynamics, 2nd Edition.* Mc-Graw-Hill, Inc, 1991.

[10] Rosema, C., et al., "MISSILE DATCOM User's Manual – 2011 Revision." AFRL-RB-WP-TR-2011-3071, March 2011. Cleared for public release: 88ABW-2011-2794.

[11] Stevens, Brian L. and Lewis, Frank L. *Aircraft Control and Simulation, 2nd edition.*

[12] Nelson, Robert C. Dr., *Flight Stability and Automatic Control.* McGraw-Hill, 1998.

[13] Picture obtained from http://www.rcgroups.com/forums/attachment.php?attachmentid=2715701

[14] Picture obtained from http://dc179.4shared.com/doc/KYkVGOV9/preview.html

[15] Murman, Scott M., and Aftosmis, Michael J. "Dynamic Analysis of Atmospheric-Entry Probes and Capsules." AIAA-2007-0074

[16] Briefing: "AVTAS Overview." AFRL/RQCD, Sept 2012. Cleared for public release: 88ABW-2012-0686.

[17] Haas, R.L., "The Large Amplitude Multi-Mode Aerospace Research (LAMAR) Simulator. AIAA-73-922.